sustainability

MDPI

Article

The Role of Cheap Chemicals Containing Oxygen Used as Diesel Fuel Additives in Reducing Carbon Footprints

Salih Özer

Department of Mechanical Engineering, Engineering and Architecture Faculty, Muş Alparslan University, 49100 Muş, Türkiye; s.ozer@alparslan.edu.tr

Abstract: This study investigates the improvement of combustion performance, engine emissions, energy, exergy, and thermodynamic efficiencies by adding oxygenated additives to diesel/biodiesel blends. Five different fuel mixtures (D100, D80B20, D50B50, D30B50S20, and D30B50G20) were tested in a diesel engine. The positive effects of the additives on engine efficiency became evident. In terms of combustion performance, the maximum in-cylinder pressure was observed with D100; however, a decrease of 11.51% was noted with the D50B50 mixture, while an increase of 7.51% was achieved with the addition of butyl diglycol. The addition of butyl diglycol also increased the heat release rate by 34.36%. Regarding exhaust emissions, the D30B50G20 fuel produced the lowest CO emissions (0.02%), while HC emissions decreased by 80% compared to D100. Smoke opacity was also found to be lower with D30B50G20. However, these additives led to a 2.65% decrease in certain performance metrics. On the other hand, the sustainability analysis revealed that the most efficient fuel mixture was D30B50G20.

Keywords: biofuels; biodiesel; canola oil; solketal; butyl diglycol; energy and exergy

check for updates

Academic Editors: Lei Zhang and Jun Wang

Received: 26 January 2025
Revised: 17 March 2025
Accepted: 22 March 2025
Published: 2 April 2025

Citation: Özer, S. The Role of Cheap Chemicals Containing Oxygen Used as Diesel Fuel Additives in Reducing Carbon Footprints. *Sustainability* **2025**, *17*, 3146. https://doi.org/10.3390/su17073146

1. Introduction

In recent years, it has been noted that the increasing use of fossil fuel sources has led to a rise in pollutant emissions and that this situation has reached levels that will cause global climate change [1]. It is believed that a significant portion of global air pollution originates from machines equipped with internal combustion engines used in the transportation sector [2]. Machines using internal combustion engines continue to be predominantly preferred across various fields, from the transportation sector to agriculture and healthcare [3]. For this reason, countries are imposing certain restrictions to reduce exhaust emissions from motor vehicles. These regulations are pushing companies and researchers to engage in production aimed at reducing emissions. Most researchers believe that these restrictions can be overcome by utilizing renewable energy sources. Therefore, there is a focus on reducing exhaust emissions by using plant or animal oils or alcohols of renewable origin in internal combustion engines [4–7].

Biodiesel has an important place in biomass-based fuels. It is a significant alternative to petroleum, which can be produced by reacting a raw material with a biomass source that has oil characteristics with alcohol. Biodiesel fuel is not dependent on geography, unlike petrol [8]. Biodiesel can be produced by growing plants such as soybean, canola, and safflower as raw materials [9]. In addition, biodiesel can be mixed with diesel fuel in any ratio [10]. The use of biodiesel is increasing due to its high cetane number and low emission values. However, researchers mention the low emission values of biodiesel. Although

this is considered a significant disadvantage, the improvement in exhaust emissions can compensate for the amount of fuel consumed [11].

In addition, due to the differences in the types of raw materials used in biodiesel production, viscosity and density values can sometimes be higher than those of diesel fuel [12]. Furthermore, the fact that biodiesel has a cloud point and freezing point at higher temperatures compared to diesel fuel can lead to the clogging of vehicle filters [13]. These issues have prompted increased research into the use of additives to enhance the viscosity, density, cloud point, and freezing point of biodiesel. Additionally, some researchers have indicated that oxygen-containing additives can improve the combustion characteristics of biodiesel and enhance combustion efficiency [14]. Xiao et al. [3] studied the effects of adding 10%, 20%, and 30% iso-butanol to pure biodiesel on engine performance and exhaust gas emissions. They reported that increasing the amount of iso-butanol added to biodiesel enhanced the evaporation and atomization of fuel mixtures, leading to improved combustion. They noted that ignition delay and combustion time decreased with a higher iso-butanol content in biodiesel. Compared to diesel fuel, in-cylinder pressure values increased with the addition of iso-butanol. While NOx emissions rose, particulate emissions decreased with the incorporation of iso-butanol. Huang et al. [2] examined the effects of adding 10% and 20% methanol to pure soybean oil biodiesel to enhance combustion efficiency. An increase in in-cylinder pressure values and heat dissipation rates was observed with the addition of methanol to biodiesel. There was a rise in HC emissions and a decrease in CO emissions with the addition of methanol. Kumar et al. [15] studied the effects of adding diethyl ether and cerium oxide (CeO_2), a nanoparticle, to biodiesel derived from waste oils on engine performance and exhaust gas emissions. They found that the additives incorporated into biodiesel increased thermal efficiency, reduced HC and soot emissions, and partially raised NOx emissions. Kumar et al. [16] conducted a study to reduce the exhaust gases of biodiesel by adding solketal. For this purpose, 9%, 10%, 12%, and 15% solketal were added to biodiesel by volume. They reported that the addition of solketal increased specific fuel consumption, elevated NOx and CO_2 emissions, and decreased HC, CO, and soot emissions. Chang et al. [17] added acetone-butanol-ethanol (ABE) to the fuel mixture to enhance the combustion efficiency of a blend of biodiesel and diesel fuel. They reported that the addition of ABE to the diesel/biodiesel fuel blend improved combustion efficiency and reduced NOx and polycyclic aromatic hydrocarbon (PAH) emissions. Şimşek and Çolak [18] investigated exhaust gas emission values and engine performance metrics by incorporating 10% and 20% propanol alcohol into biodiesel. They reported that the addition of propanol positively affected engine power and fuel consumption values. They also found that CO, NOx, and soot emissions decreased while HC emissions increased with a higher propanol ratio in fuel mixtures. Masera et al. [19] studied the effect of the addition of 15% by volume of 2-Butoxyethanol into biodiesel produced from waste frying oil and rapeseed oil to enhance the effects of its high viscosity and combustion properties on fuel characteristics, engine performance, and exhaust gas emissions. They stated that the addition of 2-Butoxyethanol improved combustion efficiency and reduced exhaust gas emissions. Nabi and Resul [20] carried out an exergy analysis using fuel blends obtained by mixing pure diesel with waste cooking oil and macadamia (Macadamia integrifolia) biodiesel. They reported that total unburnt hydrocarbons (THC), carbon monoxide (CO), and particulate matter (PM) emissions decreased, while NOX emissions increased in biodiesel/diesel fuel blends compared to pure diesel. In the study, it was explained that the highest exergy efficiency achieved was 30%. Sekmen and Yılbaşı [21] conducted an experimental study on an engine using biodiesel and pure diesel fuels, comparing these fuels through exergy analysis. They reported that the exergy efficiencies of biodiesel and diesel fuel were 28.94% and 27.52%, respectively. When the energy distribution in biodiesel was analyzed, it was

explained that exergy destruction was 47%, useful work was 28.95%, exergy loss due to heat transfer was 7.3%, and exhaust exergy was 16.7%. Odibi et al. [22] evaluated waste cooking biodiesel and diesel fuels through exergy analysis. It was explained that waste cooking biodiesel exhibited the lowest exhaust loss rate and was 6% more thermally efficient than pure diesel fuel. It was reported that very high exergy destruction of 55% occurred due to the use of waste cooking biodiesel. Yeşilyurt and Arslan [13] produced biodiesel from a mixture of waste cooking oil and canola oil and performed exergy analysis. They reported that the maximum exergy efficiency was 20.52% when biodiesel was used as fuel in the engine. Additionally, the exergy destruction of biodiesel fuel was calculated to be between 58.9% and 62.8%.

In their study, Paul et al. [23] used ternary fuel blends obtained from diesel, ethanol, and Pongamia pinnata methyl ester (PPME) fuels in various ratios. It was stated that exergy efficiency increased with rising engine load for all fuel blends. It was explained that the highest exergy efficiency was achieved at 31% with D35E15B50 fuel. Furthermore, it was noted that D35E15B50 fuel exhibited a 22.02% reduction in exergy destruction rate and a 21.06% reduction in entropy production rate compared to pure diesel fuel. Madheshiya and Vedrtnam [24] conducted an experimental study using biodiesel derived from waste cooking oil/mustard oil and pure diesel fuels. The exergetic evaluation of these fuel blends was performed using the results obtained in the experimental study. It was reported that biodiesel fuels demonstrate significant energy performance when utilized as an alternative to diesel fuel. It was stated that the cooling water exergy of WCO30 fuel is 5% higher than that of pure diesel fuel. Kul and Kahraman [25] conducted experimental studies utilizing diesel, biodiesel, and bioethanol fuels in different ratios within a compression ignition engine. Exergy analysis was conducted using the results obtained from the experimental study. At an engine speed of 1400 rpm, the maximum thermal efficiency was 31.42% for D100 fuel and 28.68% for D92B3E5 fuel. Hoseinpour et al. [26] performed an exergy analysis using data obtained from tests on a compression ignition engine using waste cooking oil, biodiesel, and diesel blends. It was reported that thermal and exergy efficiencies increased with increasing engine load for all fuel blends. The highest exergy efficiency was calculated at 42% for B20 fuel at a pressure of 6 bar. Sanli and Uludamar [27] carried out an exergy analysis in a diesel engine utilizing pure diesel, biodiesel made from hazelnut oil, and biodiesel derived from canola oil. The lowest exergy destruction in canola biodiesel was reported as 47.41% at an engine speed of 1800 rpm. At the same engine speed, the lowest entropy production was 0.15 kW/K in canola biodiesel. Khoobbakht et al. [28] investigated the exergy efficiency at different engine speeds using triple-fuel blends comprising diesel, biodiesel, and ethanol fuels. According to the results from the energy and exergy analyses obtained in the study, it was reported that 43.09% of the fuel exergy was destroyed, with the average thermal efficiency being approximately 36.61% and the exergy efficiency being approximately 33.81%.

The literature summary indicates that researchers have focused on the effects of additives added to fuel to improve the fuel properties of biodiesel. Additionally, it has been determined that the mixing of oxygen-rich substances (such as butanol, ethanol, methanol, etc.) or solvents (such as heptane, hexane, and diethyl ether) affects the exhaust gas emissions and performance characteristics of biodiesel. Solketal is an oxygen-rich fuel, and butyl diglycol is a solvent with a high calorific value and cetane number. Limited research has been conducted on the effects of adding solketal and butyl diglycol to biodiesel fuel concerning performance, combustion, and emission characteristics. Furthermore, studies conducted on biodiesel have reported that a mixture of 20% biodiesel with diesel fuel (D80B20) yields the best results concerning engine performance, fuel consumption, and exhaust gas emissions [29–31]. This study aims to increase combustion efficiency and

reduce harmful exhaust emissions by adding various additives to a D50B50 fuel, which is achieved by adding a higher proportion (50%) of biodiesel to diesel fuel. It has also been determined that energy and exergy analysis studies have not been carried out to evaluate the effects of solketal and butyl diglycol additives on engine performance characteristics in internal combustion engines. For this purpose, different fuel mixtures (D100, D80B20, D50B50, D30B50S20, and D30B50G20) were prepared using diesel, canola biodiesel, solketal, and butyl diglycol, and their effects on engine performance characteristics were investigated in detail. Engine tests were repeated for each fuel mixture at an engine speed of 3000 rpm under motor loads of 1.6 Nm, 3.2 Nm, 4.8 Nm, 6.4 Nm, 7.9 Nm, 9.5 Nm, and 11.1 Nm. During the engine tests, pressure values in the cylinder and fuel line, exhaust emission values, brake-specific fuel consumption, and exhaust gas temperature values were recorded. Additionally, energy and exergy analyses were conducted using data obtained from the experimental studies.

2. Materials and Methods

2.1. Biodiesel Generation

In this study, canola oil biodiesel, solketal, and butyl diglycol were blended with diesel fuel. Diesel fuel was purchased from a local OPET gas station, and canola oil was obtained from a nearby market. The transesterification method, which is widely utilized in biodiesel production, was applied. The transesterification reaction was carried out using 20% by volume (v/v) methanol and 0.5% by weight (w/w) NaOH. The reaction temperature was 60 °C, the reaction time was 1.5 h, and the stirring speed was 800 rpm. At the end of the reaction, biodiesel and glycerin phases were separated after allowing the mixture to rest in a separatory funnel for 12 h. The obtained biodiesel was washed three times with distilled water at 55 °C. The biodiesel was dried at 110 °C for 1 h to remove any remaining water.

The test fuels used in the experimental studies conducted within this scope consist of 80% diesel fuel–20% canola oil biodiesel (D80B20), 50% diesel fuel–50% canola oil biodiesel (D50B50), 30% diesel fuel–50% canola oil biodiesel–20% solketal (D50B50S20), and 30% diesel fuel–50% canola oil biodiesel–20% butyl diglycol (D50B50G20). The detailed ratios of the mixtures and the abbreviations used in the graphs are presented in Table 1. Some properties of the test fuels were determined at the Scientific and Technological Research Council of Turkey—Marmara Research Centre (TUBITAK-MAM) and are shown in Table 2.

Table 1. The blending concentrations of the test fuels.

No	Abbreviation	Diesel	Biodiesel	Solketal	Butyl Diglycol
1	D100	100%	-	-	-
2	D80B20	80%	20%	-	-
3	D50B50	50%	50%	-	-
4	D30B50S20	30%	50%	20%	-
5	D30B50G20	30%	50%	-	20%

Table 2. The properties of test fuels.

Fuels	Density (15 °C, kg/m^3)	Viscosity (40 °C, mm^2/s)	Thermal Value (MJ/kg)	Flash Point (°C)	Cetane Number
Test Method	ASTM D4052	ASTM D445	ASTM D240	ASTM D93	-
Diesel	831.7	2.58	45.98	63	56
Biodiesel	890	3.9	40.01	140	58.6

Table 2. *Cont.*

Fuels	Density (15 °C, kg/m^3)	Viscosity (40 °C, mm^2/s)	Thermal Value (MJ/kg)	Flash Point (°C)	Cetane Number
Solketal *	1071.1	5.21	25.91	84	-
Butyl diglycol **	960.6	3.654	32.0	99	54
D80B20	843.36	2.844	44.786	78.4	56.52
D50B50	860.85	3.24	42.995	101.5	57.3
D30B50S20	908.73	3.766	38.981	105.7	-
D30B50G20	886.63	3.4548	40.199	108.7	56.9

* Ref. [32]. ** CAS-No:112-34-5.

2.2. Experimental Setup

In the experimental study, a naturally aspirated, four-stroke, air-cooled, single-cylinder, compression-ignition (CI), direct-injection (DI) diesel engine was used. The main characteristics of the diesel engine used in this study are shown in Table 3.

Table 3. The technical specifications of the diesel engine used in the experimental studies.

Diesel Engine	
Parameters	**Specifications**
Model	186 FAG
Number of cycles	4
Number of cylinders	1
Maximum engine power	7 kW (3600 rpm)
Type of fuel	Diesel fuel
Type of ignition	Compression ignition
Type of fuel injection	Direct injection
Intake system	Naturally aspirated
Engine speed	3000 rpm
Swept volume	418 cm^3
Stroke	70 mm
Bore	86 mm
Cooling system	Air-cooled
Injector nozzle number	4
Pressure of injection	19.6 ± 0.49 Mpa
Fuel delivery advance angle	22 ± 1 (°CA) BTDC
Compression ratio	18:1

All tests within the scope of this study were conducted at a constant speed of 3000 rpm and with different engine loads (1.6 Nm, 3.2 Nm, 4.8 Nm, 6.4 Nm, 7.9 Nm, 9.5 Nm, and 11.1 Nm). Fuel consumption was determined by mass using an electronic scale with an accuracy of 0.01 g. In-cylinder pressure values were measured with a Kistler 4065B0200DS1 model pressure sensor. Fuel line pressure was measured using an Oprant AutoPSI-A model pressure sensor. The crankshaft position was determined by an FNC 50B incremental optical encoder. Exhaust gas temperature was measured using a K-type thermocouple. Data from the sensors were collected using a 4-channel PicoScope 2406B

oscilloscope. Each in-cylinder pressure and fuel line pressure value was obtained by averaging 100 cycles with 0.25 °CA precision. The heat release rate for each crank angle was calculated using Equation (1).

$$\frac{dQ}{d\varnothing} = \frac{k}{k-1}\left(P\frac{dV}{d\varnothing}\right) + \frac{1}{k-1}\left(V\frac{dP}{d\varnothing}\right) \quad (1)$$

where $dQ/d\varnothing$ is the heat release rate (J/KMA), k is the ratio of specific heats (Cp/Cv), P is the cylinder pressure (Pa), and V is the variable cylinder volume (m^3).

A Mobydic 5000 COMBI exhaust emission device was used to measure exhaust emissions. The technical specifications of the exhaust emission device are presented in Table 4. The schematic view of the experimental setup is given in Figure 1.

Table 4. Technical properties of the exhaust emissions device.

Measurement	Measuring Range	Resolution	Precision
CO (% vol)	0–10	0.01	±1%
CO_2 (% vol)	0–20	0.01	±0.5%
HC (ppm)	0–20,000	1	±12
NO_X (ppm)	0–5000	1	±10
O_2 (% vol)	0–21	0.01	±0.5%
Smoke opacity (%)	0–20	0.01	±2

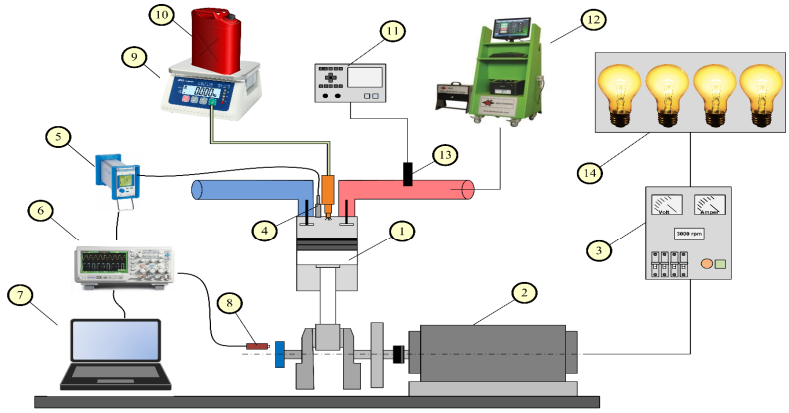

Figure 1. Experimental setup [33].

2.3. Thermodynamic Analysis

In these engine experiments, a diesel engine consistently operated at 3000 rpm while varying the load in increments of 1 kW, ranging from 1 kW up to 5 kW. Fuel consumption was measured by timing how long it took for the engine to consume 10 g of fuel, using a highly precise electronic scale with an accuracy of 0.01 g. The exhaust gas temperature was monitored using a K-type thermocouple. Emissions of hydrocarbons (HCs), carbon monoxide (CO), carbon dioxide (CO_2), and smoke were analyzed utilizing a Mobydic 5000 COMBI exhaust gas analyzer. The experimental studies were carried out under dynamic test conditions to evaluate engine performance and emissions based on thermodynamic principles. The following assumptions were made:

1. The gases entering and exiting the cylinder are assumed to behave as ideal gases;
2. The temperature of the cylinder walls remains constant during the experiments;
3. Ambient conditions are maintained at 20 °C and atmospheric pressure (1 atm);

4. The engine is assumed to operate under continuous, steady-state conditions.

Technical specifications and uncertainty analyses of the measurement devices are detailed in Table 4. A schematic diagram of the experimental setup is presented in Figure 2.

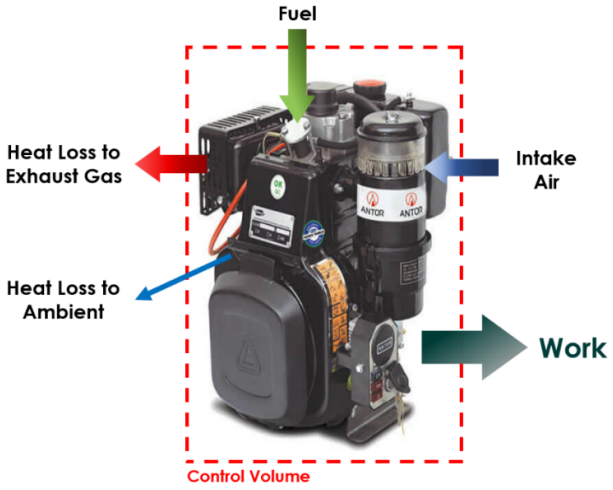

Figure 2. Control volume for thermodynamic analyses [33].

2.4. Energy Analysis

The total amount of energy in internal combustion engines consists of the sum of kinetic (e_{kn}), potential (e_{pt}), physical (e_{phy}), and chemical (e_{chm}) energies. In this study, kinetic and potential energies in the control volume were neglected [34].

$$e = e_{kn} + e_{pt} + e_{phy} + e_{chm} \tag{2}$$

Physical energy is the sum of internal and flow energies. This sum is expressed with enthalpy (h). In this study, the variation of specific heat (c_p) with temperature at constant pressure was neglected. For burn gases, chemical energy is equal to the sum of the enthalpy of gas formation and its physical enthalpy [34].

$$e_{phy} = u + pv \tag{3}$$

$$h_2 - h_1 = c_p(T_2 + T_1) \tag{4}$$

The energy balance can be written according to the first law of thermodynamics, or in other words, the conservation of energy principle, for a control volume given in Figure 1 [33].

$$\left(\dot{Q}_{in} - \dot{Q}_{out}\right) + \left(\dot{W}_{in} - \dot{W}_{out}\right) = \sum \dot{m}_{out} h_{out} - \sum \dot{m}_{in} h_{in} \tag{5}$$

The energy generated per unit time as a result of the combustion of blends in the cylinder was calculated with the following expression using the lower heating value (H_u) and mass flow rate ($\dot{m}_{fuel}$) of the fuel [35].

$$\dot{E}_{fuel} = \dot{m}_{fuel} H_u \tag{6}$$

The engine's output power is measured using a dynamometer during the tests. Thermal losses can be found using power and energy flows [36]. Furthermore, the exhaust

energy was calculated using the mass flow rates of the emissions released from the engine into the environment in this study.

$$\dot{Q}_{lost} = \dot{E}_{fuel} - \dot{W} \tag{7}$$

Thermal efficiency is the ratio of the engine's output power to fuel energy. It shows how much useful work is obtained from the energy of fuel blends entering the engine [37–39].

$$\eta = \frac{\dot{W}}{\dot{E}_{fuel}} \tag{8}$$

2.5. Exergy Analysis

Based on the second law of thermodynamics, energy conversion and heat transfer between energy sources and systems are inherently limited in efficiency. In this framework, exergy serves as a key indicator, quantifying the portion of transferred energy that can be converted into useful work. The exergy balance is expressed as follows [40].

$$\dot{E}x_{air} + \dot{E}x_{fuel} = \dot{E}x_{w} + \dot{E}x_{ex} + \dot{E}x_{heat} + \dot{E}x_{dest} \tag{9}$$

Fuel exergy ($\dot{E}x_{fuel}$), the exergy of heat lost from the engine body ($\dot{E}x_{heat}$), the exergy of exhaust gases released into the environment, and exergy ($\dot{E}x_{ex}$) destruction are key components in exergy analysis. Since the air entering the engine is sourced directly from the environment, its exergy contribution is assumed to be zero [41]. The exergetic power ($\dot{E}x_{w}$) corresponds to the engine's output power. The exergy of liquid fuel is determined using the following equation [42].

$$\dot{E}_{fuel} = \dot{m}_{fuel}\varphi LHV_{fuel} \tag{10}$$

Here, (φ) is the exergy factor. The exergy factor is calculated using the data obtained by analyzing the fuel [43].

$$\varphi = 1.0401 + 0.1728\frac{h}{c} + 0.0432\frac{o}{c} + 0.2169\frac{\alpha}{c}\left(1 - 2.0628\frac{h}{c}\right) \tag{11}$$

Calculating the exhaust exergy is a complex step in exergy analysis. It begins with measuring emissions, followed by formulating the actual combustion equation based on the proportions of fuel, air, and emissions. From this equation, the mole fraction of each gas is determined. The total exhaust gas flow rate ($\dot{m}_{total}$) is estimated as 98% of the fuel flow rate entering the control volume [44]. The exhaust gas exergy is then calculated by summing the physical exergy (ε_p) and chemical exergy (ε_c) of each component.

$$\dot{E}x_{ex,i} = \sum\left(\varepsilon_p + \varepsilon_c\right)_i \tag{12}$$

Chemical and physical exergies were calculated using the equations given in Equations (10) and (11) [45].

$$\varepsilon_p = [\,(h - T_0 s) - (h_0 - T_0 s_0)] \tag{13}$$

$$\varepsilon_{ch} = \overline{R}T_0 ln\frac{1}{y^e} \tag{14}$$

The chemical exergy calculations were based on the literature values for atmospheric gas percentages (y^e) [46]. Furthermore, the temperature of the engine casing was recorded

during the experiments to determine the exergy of heat transferred from the engine casing to the surroundings, as described in Equation (14) [47].

$$\dot{E}x_{heat} = \sum \left(1 - \frac{T_0}{T_s}\right) \dot{Q}_{loss} \tag{15}$$

where (T_s) is the engine casing temperature. The entropy produced can be determined according to Equation (15) given below [48].

$$\dot{s}_{gen} = \frac{\dot{E}x_{dest}}{T_0} \tag{16}$$

Exergy efficiency, calculated using Equation (16) [49], represents the ratio between the system's input and output exergy values. This metric provides insight into how effectively the energy within the system is converted into useful work.

$$\eta_{ex} = \frac{\dot{E}x_W}{\dot{E}x_{in}} \tag{17}$$

3. Results and Discussion

3.1. Combustion Characteristics

In-cylinder pressure curves are an important parameter for understanding the effectiveness of fuels in alternative fuel studies. In this section, heat dissipation, cumulative heat generation, and pressure increase rates calculated using in-cylinder pressure values are analyzed in detail. The in-cylinder pressure values of each test fuel for different engine loads are presented in Figure 3. The in-cylinder pressure values decreased with the addition of biodiesel to diesel fuel. Considering all engine loads, the average reduction in in-cylinder pressure compared to D100 fuel was 7.44% with D80B20 and 11.51% with D50B50 fuels, respectively. Biodiesel has a higher viscosity and lower volatility than diesel fuel. This results in poor atomization of the fuel and an inadequate air–fuel mixture, which reduces the maximum in-cylinder pressure values [50]. Similar results were obtained by refs. [51,52].

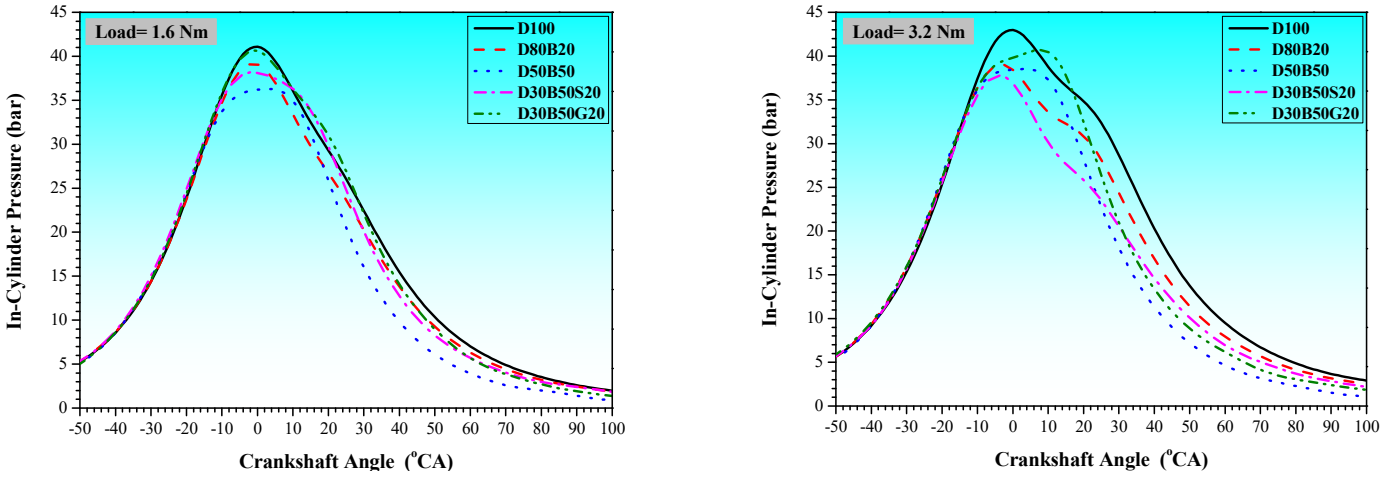

Figure 3. *Cont.*

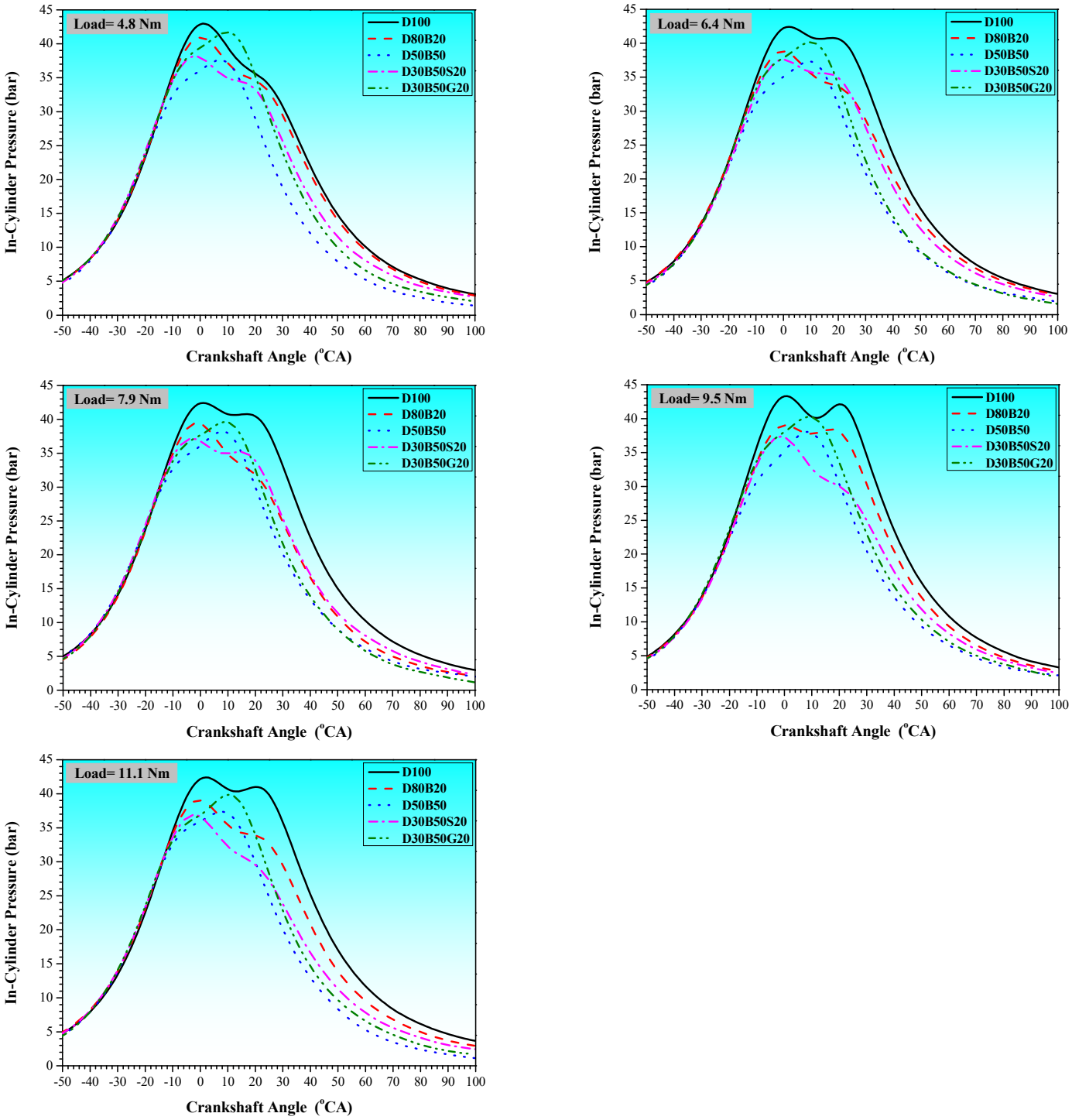

Figure 3. The variation in cylinder pressures depending on the crankshaft angle.

With the addition of butyl diglycol to the D50B50 fuel mixture, in-cylinder pressure values increased for each engine load. The average increase in in-cylinder pressure with the addition of butyl diglycol was 7.51%. Considering all test fuels, the highest in-cylinder pressure value for each engine load was recorded with D100 fuel, while the second-highest in-cylinder pressure values were achieved with the D30B50G20 fuel blend. The calorific values of the blended fuels used in the tests are lower than those of diesel fuel (Table 1). Studies have reported that fuels with lower calorific values lead to reduced in-cylinder pressure values [53]. The reason for the higher in-cylinder pressure values obtained with the addition of solketal and butyl diglycol to the D50B50 fuel mixture can be attributed to the

increase in the oxygen content of the mixture due to these additives and the improvement in viscosity and density values. It is reported that oxygen-rich fuels exhibit better combustion performance and higher in-cylinder pressure values [54].

Figure 4 shows the heat release values of each test fuel at different engine loads. The highest heat release values for each engine load were achieved with D100 fuel. Lower heat release values were obtained with D80B20 and D50B50 fuels compared to D100 fuel. Due to the higher viscosity and lower calorific value of biodiesel compared to diesel fuel, it exhibits a lower heat release value [55]. The addition of solketal and butyl diglycol to D50B50 fuel increased the heat release rate. Considering all engine loads, the average increase in the heat release rate with the addition of solketal and butyl diglycol was 19.78% and 34.36%, respectively, compared to D50B50 fuel. Higher heat release values were obtained with the butyl diglycol additive than with the solketal additive; the highest heat release values were recorded with the D30B50G20 fuel blend after D100 fuel. Studies have reported that oxygen-rich fuel blends result in higher heat release values by enhancing combustion in the premixed combustion phase [56,57].

Figure 5 shows the cumulative heat release values of each test fuel for different engine loads. The highest cumulative heat generation value was obtained with D100 fuel at all engine loads. Similar to the heat release results, lower cumulative heat release was obtained with diesel/biodiesel fuel blends (D80B20 and D50B50) compared to D100 fuel. At all engine loads, the lowest cumulative heat generation value was calculated as 308.34 J with the D50B50 fuel blend and an engine load of 1.6 Nm, while the highest value was calculated as 931.19 J with D100 fuel at an engine load of 11.1 Nm. The low cumulative heat generation with diesel/biodiesel fuel blends can be attributed to their high viscosity, high density, and low thermal energy content [58]. The addition of solketal and butyl diglycol to the diesel/biodiesel fuel blend (D50B50) resulted in an increase in cumulative heat generation. The average increase in cumulative heat release for each engine load was calculated as 33.6% and 34.8% for the additions of solketal and butyl diglycol, respectively. Again, similar to the heat release rates, slightly higher cumulative heat release was obtained with the addition of butyl diglycol compared to solketal. The higher cumulative heat release is believed to result from better combustion due to the oxygen content of the fuel blends [59].

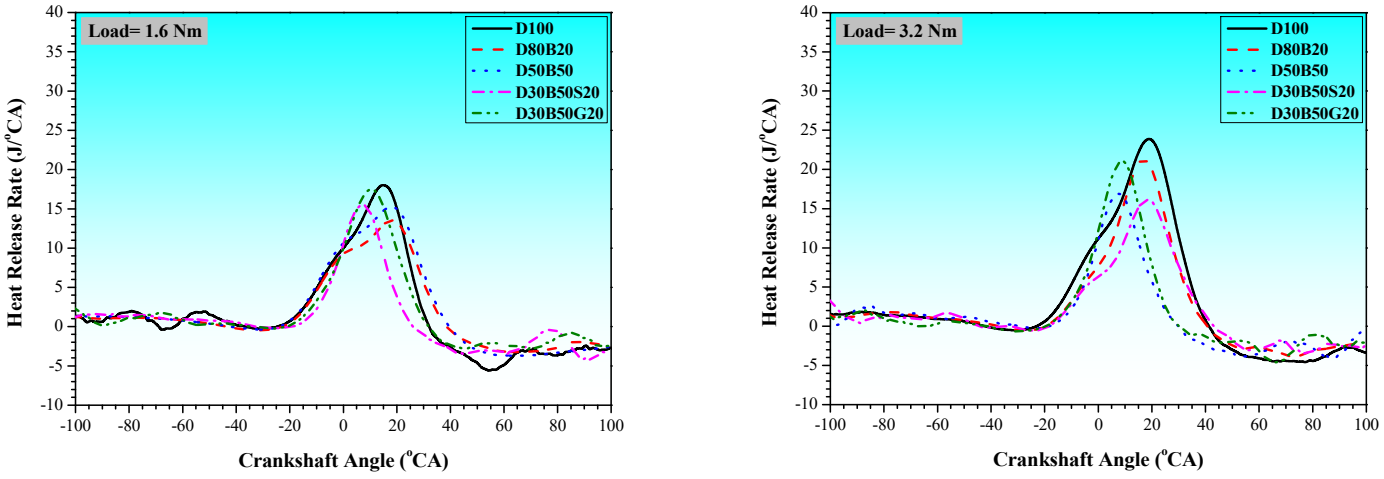

Figure 4. *Cont.*

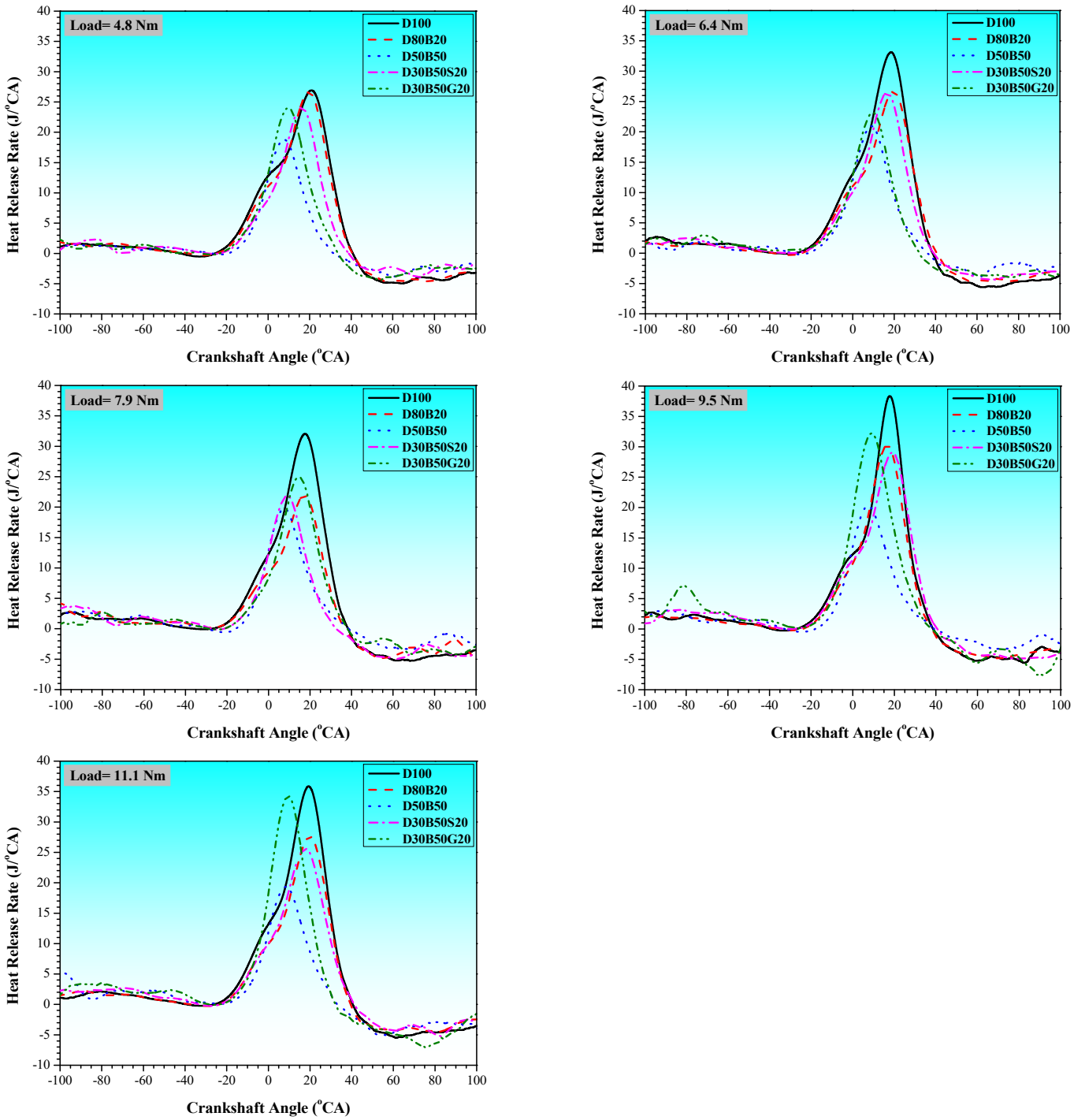

Figure 4. The variation in the heat release rate (HRR) depending on the crankshaft angle.

Figure 6 shows the rate of pressure rise (ROPR) values for each test fuel. As can be seen from Figure 5, the peak ROPR value generally increased due to the increase in the amount of fuel taken into the cylinders with increasing loads. Compared to diesel fuel, the ROPR value decreased with diesel/biodiesel fuel blends. Considering all engine loads, the average reduction in the ROPR value compared to diesel fuel was 6.35% with the D80B20 fuel and 15.94% with the D50B50 fuel. Diesel fuel possesses a higher heating value and longer ignition delay than D80B20 and D50B50 fuels. Due to the longer ignition delay, more fuel accumulates in the combustion chamber, resulting in higher obtained ROPR values from the sudden combustion of a large amount of fuel [60]. An increase in the ROPR value occurred with the addition of solketal and butyl diglycol to the D50B50 fuel blend.

With the D30B50S20 and D30B50G20 fuel blends, the average increase in the ROPR value compared to D50B50 fuel was recorded as 8.38% and 10.13%, respectively. According to the results obtained, it was observed that the addition of butyl diglycol resulted in higher ROPR values than the addition of solketal.

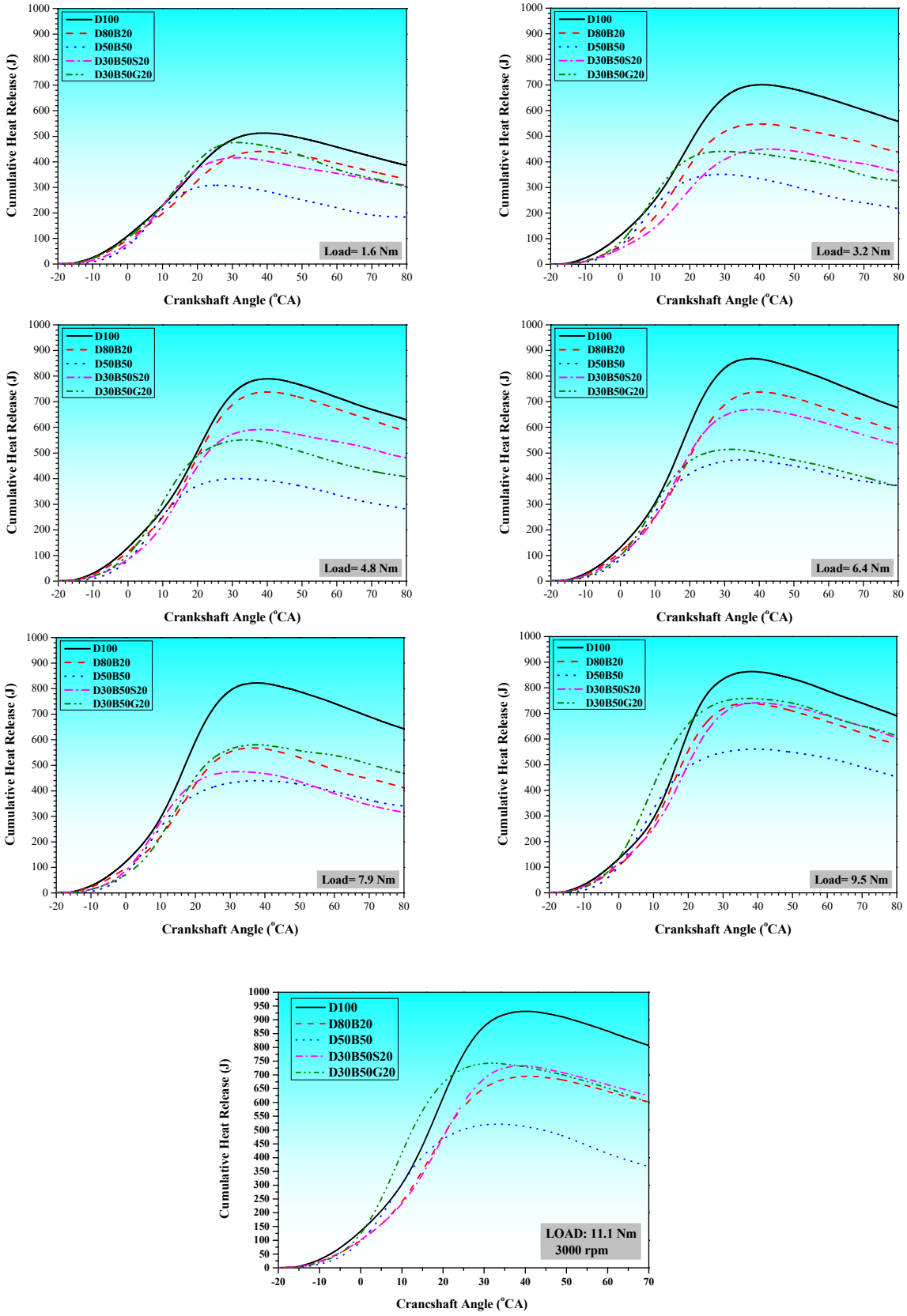

Figure 5. The variation in cumulative heat release (CHR) depending on the crankshaft angle.

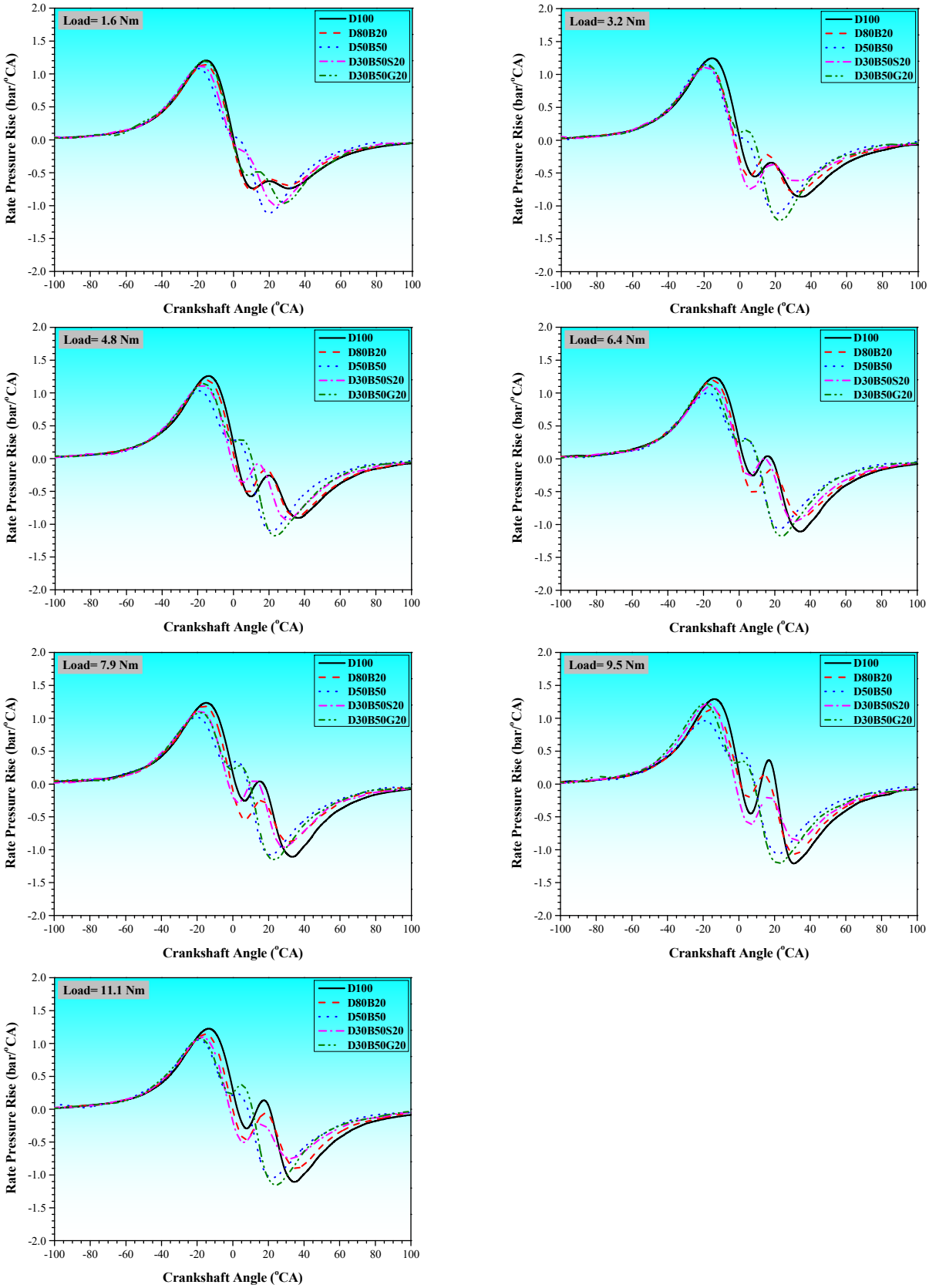

Figure 6. The variation in the rate of pressure rise (RoPR) depending on the crankshaft angle.

The reason for the higher ROPR values obtained with the addition of solketal and butyl diglycol is the high oxygen content, low viscosity, and flash point of the mixture (see Table 1). Thus, better volatility and fuel atomization are achieved. Additionally, the oxygen

content of the mixture is thought to accelerate combustion [61], leading to an increasing trend in the rate of pressure build-up.

The exhaust gas temperature values of each test fuel for different engine loads are provided in Figure 7. Exhaust gas is an indicator of combustion inside the cylinder in internal combustion engines. In Figure 7, it was observed that the exhaust gas temperature (EGT) decreased with the D80B20 and D50B50 fuel blends compared to diesel fuel. With the addition of biodiesel to D100 fuel, the calorific value of the fuel blends decreases. Consequently, the combustion temperature decreases, resulting in lower EGT values [62]. Similar results were obtained by refs. [63,64]. EGT values increased with the addition of solketal and butyl diglycol to D80B20 and D50B50 fuels. The oxygen content of solketal and butyl diglycol is viewed as an important parameter that causes the exhaust gas temperature to rise [45]. The lowest exhaust gas temperature recorded was 232 °C with B50D50 fuel at an engine load of 1.6 Nm, while the highest temperature value reached 443 °C with B30D50G20 fuel. The closest EGT value to B30D50G20 fuel was 431 °C with D100 fuel at an engine load of 11.1 Nm.

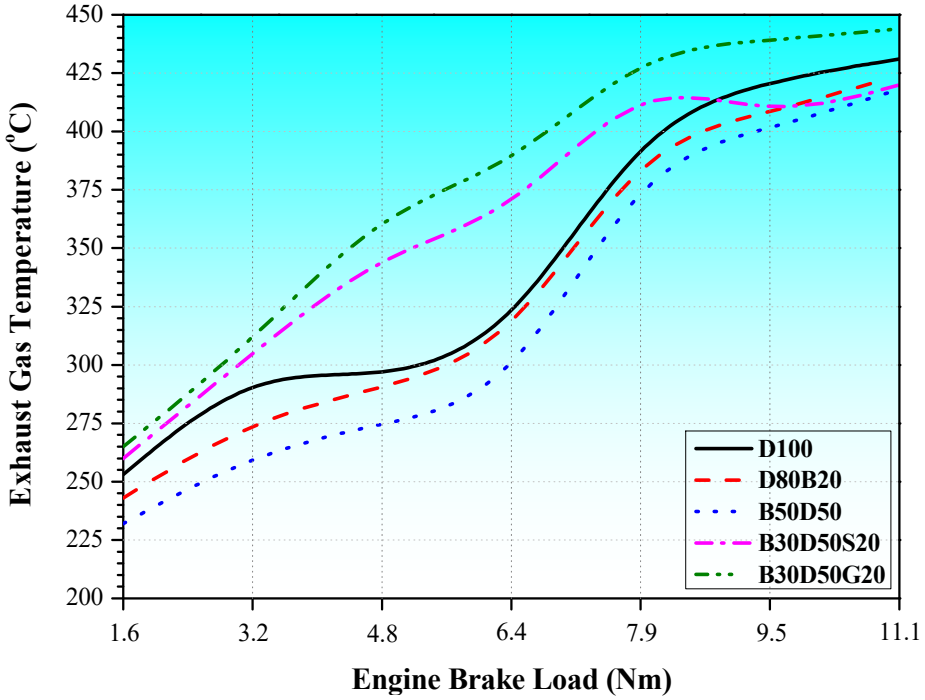

Figure 7. The variation in the exhaust gas temperature depending on the engine brake load.

The brake-specific fuel consumption values for each test fuel are presented in Figure 8 for different engine loads. The specific fuel consumption value denotes the amount of fuel consumed for 1 kWh of useful work in internal combustion engines [64]. As shown in Figure 8, specific fuel consumption decreased with increasing engine load for each test fuel. Specific fuel consumption increased with diesel/biodiesel fuel blends (D80B20 and D50B50) compared to D100 fuel. It also rose with increasing biodiesel content in the blend ratio, with the highest specific fuel consumption values for each engine load generally occurring with D50B50 fuel. Biodiesel fuel has lower heating values than diesel fuel. To achieve the same power output, more fuel is delivered into the cylinder, thus raising the specific fuel consumption [65]. Additionally, the deterioration of fuel atomization due to the high viscosity of the fuels is also cited as a reason for the high specific fuel consumption [66].

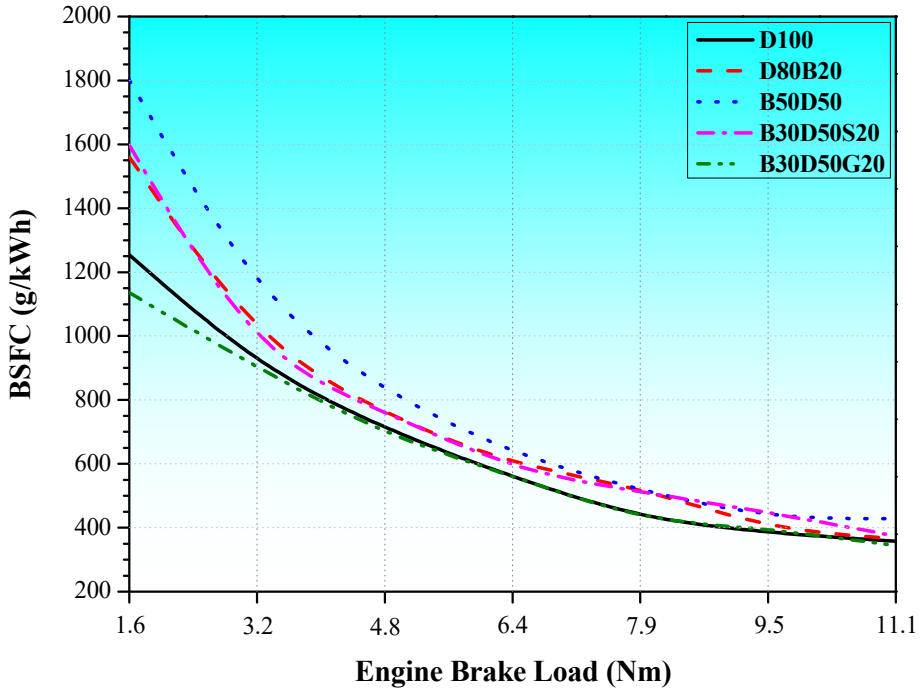

Figure 8. The variation in brake-specific fuel consumption depending on the engine brake load.

The addition of solketal and butyl diglycol to D50B50 fuel resulted in a reduction in specific fuel consumption for each engine load. The butyl diglycol additive exhibited lower specific fuel consumption than the solketal additive. In general, the specific fuel consumption values obtained with B30D50G20 fuel were below those obtained with D100 fuel. Since solketal and butyl diglycol are oxygen-containing chemicals, they partially enhance combustion, leading to lower specific fuel consumption [45].

3.2. Exhaust Emissions

Figure 9 shows the variation in carbon monoxide (CO) emissions for each test fuel. CO emissions occur as a result of the incomplete combustion of fuel in the cylinder. Many studies explain the incomplete combustion of fuel by the lack of oxygen in the cylinder and the presence of cold regions on the cylinder walls [67,68]. In Figure 9, it was observed that diesel fuel exhibited higher CO emissions than the other test fuels. Up to an engine load of 6.4 Nm, the reduction in CO emissions was greater with a higher biodiesel blend ratio in diesel fuel. At higher engine loads, CO emissions increased slightly with a higher biodiesel blend ratio. The addition of solketal to the diesel/biodiesel blend caused an increase in CO emissions up to an engine load of 6.4 Nm; after this point, CO emissions tended to decrease with increasing engine load. The butyl diglycol additive caused a decrease in CO emissions at all engine loads, with the lowest CO emission values obtained from the D30B50G20 fuel. Oxygen-rich fuels are reported to oxidize more carbon (C) atoms in the cylinder, increasing CO_2 emissions and reducing CO emissions [69]. Therefore, it is expected that CO emissions decrease with the oxygen content of biodiesel compared to D100 fuel. Similarly, solketal and butyl diglycol are chemicals with oxygen content. Additionally, butyl diglycol improved the viscosity and flash point values, while solketal enhanced the flash point values of the fuel (Table 1). Improved viscosity and flash point values are thought to partially enhance combustion and reduce CO emissions. It has been found in similar studies that CO emissions improved with the addition of oxygen-rich additives to biodiesel [70].

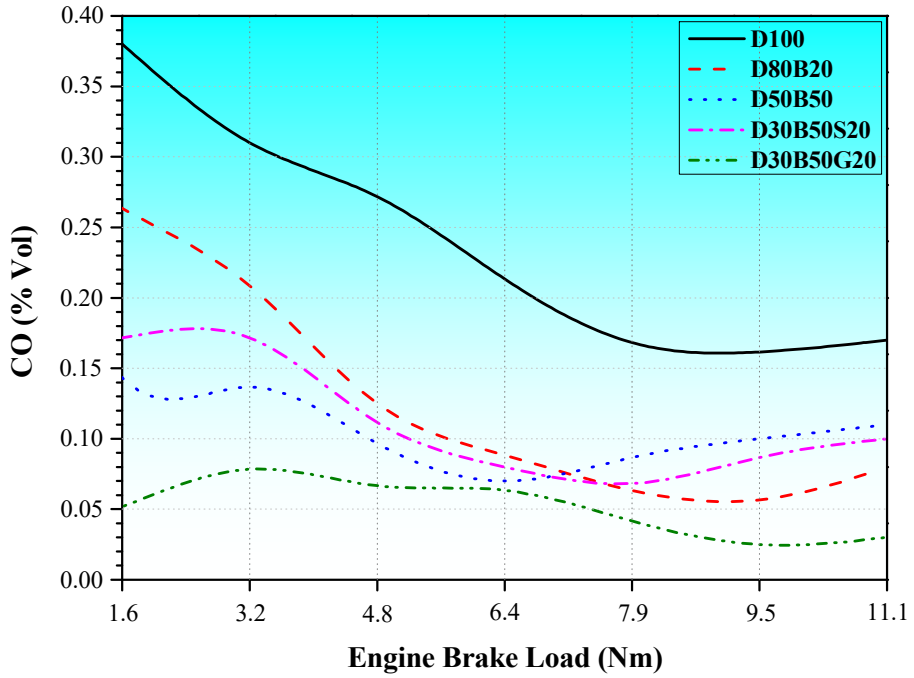

Figure 9. The variation in carbon monoxide (CO) emissions depending on the engine brake load.

Carbon dioxide (CO_2) emission values for each test fuel at different engine loads are presented in Figure 10. According to many researchers, CO_2 emissions vary based on the combustion efficiency in the cylinder [71]. In Figure 10, it was observed that the addition of solketal and butyl diglycol to the diesel/biodiesel blend resulted in high CO_2 emissions. The highest CO_2 value of 2.65% was recorded with D30B50G20 fuel at an engine load of 4.8 Nm. It is indicated that the use of oxygen-rich fuels leads to improved combustion in the cylinder, thereby increasing CO_2 emissions [72]. Furthermore, it is noted that the increased cetane number of the fuel partially advances combustion and extends the total combustion time, thus allowing CO emissions to be converted into more CO_2 emissions [73]. These results are consistent with those obtained in ref. [19].

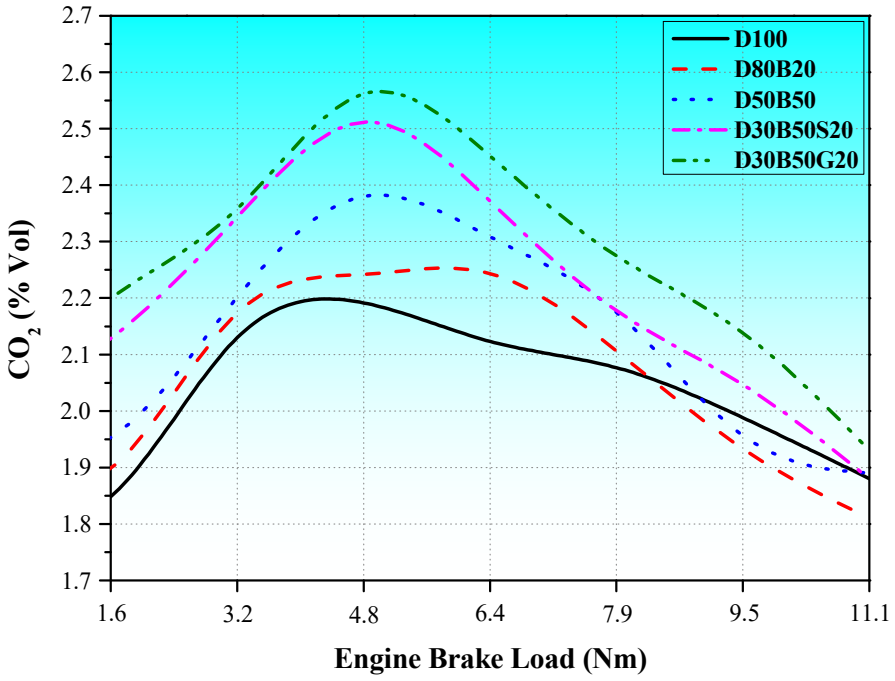

Figure 10. The variation in carbon dioxide (CO_2) emissions depending on the engine brake load.

Figure 11 shows the variation in hydrocarbon (HC) emission values for all test fuels as a function of engine load. In internal combustion engines, HC emissions are generated by the expulsion of fuel in the cylinder without complete combustion. Figure 11 indicates that the highest HC emission values for all engine loads were obtained with D100 fuel. The addition of biodiesel to diesel fuel caused a decrease in HC emissions. The reduction in HC emissions with D80B20 and D50B50 fuel blends can be explained by the increased cetane number and oxygen content of the fuel blends. An increased cetane number enhances the combustion tendency of fuel blends, and the higher oxygen content facilitates the oxidation of more fuel within the cylinder, resulting in reduced HC emissions [74]. The addition of solketal and butyl diglycol to the diesel/biodiesel blend further reduced HC emissions, and the lowest HC emission values were obtained with the butyl diglycol additive. Solketal and butyl diglycol are oxygen-containing additives. By adding solketal and butyl diglycol to the diesel–biodiesel binary-fuel blend, HC emissions reached their lowest levels due to the increased oxygen content of the blend. Similar results can be found in the literature [19,75].

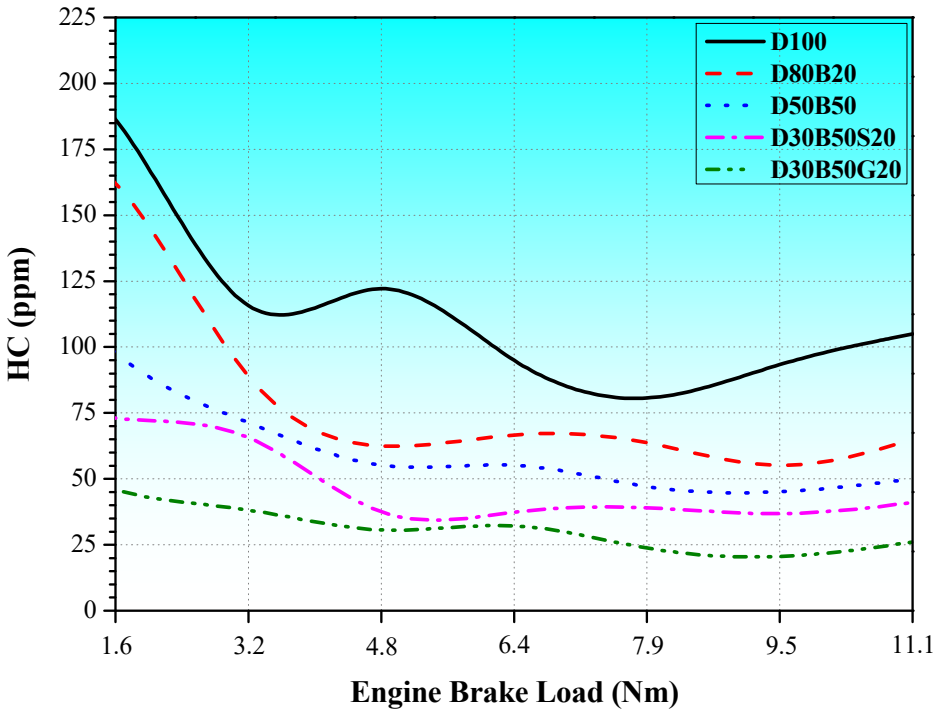

Figure 11. The variation in hydrocarbon (HC) emissions depending on the engine brake load.

Figure 12 shows the variation in the smoke emission values of each test fuel as a function of engine load. Smoke emissions are stated to be caused by a lack of oxygen in the cylinder and flame extinction near the cold cylinder walls [76]. Diesel/biodiesel binary-fuel blends exhibited lower smoke emissions than pure diesel. Biodiesel reduces smoke emissions by contributing to complete combustion with its high oxygen content [55].

The addition of solketal to the diesel/biodiesel fuel blend caused a slight increase in smoke emissions. The high density and viscosity of solketal increase the density and viscosity of the diesel/biodiesel blend. This can adversely affect the homogeneous air–fuel mixture and ultimately combustion. Therefore, it is thought to reduce the positive effect of the oxygen content of the fuel mixture, leading to increased soot emissions. On the other hand, the addition of butyl diglycol to the diesel/biodiesel fuel blend reduced smoke emissions. For each engine load, the highest smoke emission values were obtained with D100 fuel while the lowest smoke emission values were obtained with D30B50G20

fuel. Oxygen enrichment increases the oxygen/fuel ratio, improves fuel oxidation, and ultimately reduces smoke formation [77]. Similar results were obtained by ref. [78].

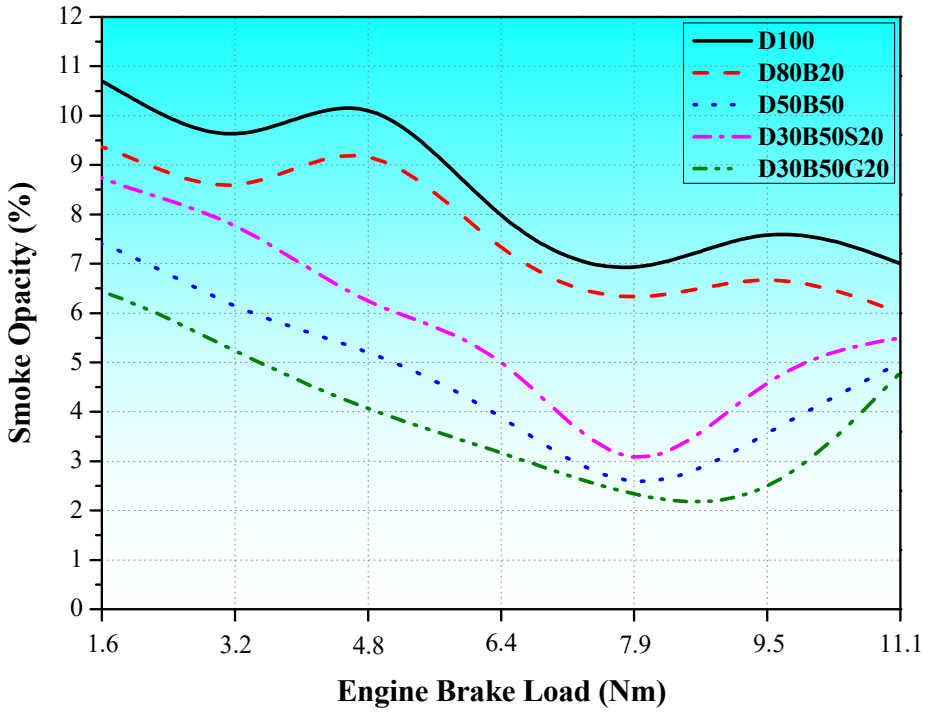

Figure 12. The variation in smoke opacity emissions depending on the engine brake load.

3.3. Energy and Exergy Analyses

In this study, the energy of the fuels entering the cylinder is calculated and given in Table 5. Fuel consumption and lower heating value determine the energy of the fuels. D50B50 fuel has the highest fuel energy at all engine torque values. The lower heating value of D50B50 fuel is lower than D100 fuel. However, since the fuel consumption of the D50B50 fuel mixture is higher, its energy is higher. Fuel energy decreases with the addition of solketal and butyl diglycol to diesel blends. With the addition of solketal, the lower heating value of the fuel blend decreases compared to D100 fuel, but fuel consumption increases. The D30B50G20 fuel blend has a higher lower heating value but lower fuel consumption than the D30B50S20 fuel blend.

Table 5. The energy flow of fuel mixtures.

Engine Brake Load (Nm)	Energy Flow (kW)				
	D100	**D80B20**	**D50B50**	**D30B50S20**	**D30B50G20**
1.6	8.010	9.704	10.577	8.649	7.117
3.2	11.567	12.154	13.131	10.034	11.275
4.8	13.559	14.066	14.485	12.414	12.952
6.4	14.257	14.791	14.783	12.530	14.114
7.9	13.689	16.441	15.176	13.867	13.186
9.5	14.704	14.665	15.100	14.589	14.954
11.1	15.974	15.972	17.601	14.175	15.046

The thermal efficiencies of the fuel mixtures used in the engine are given in Figure 13. Thermal efficiency increases for all fuel blends with increasing engine torque. The power

obtained from the engine and the energy of the fuel has a positive effect on thermal efficiency. At all brake power values, the thermal efficiencies of D30B50S20 and D30B50G20 fuels are higher than the D100 fuel and biodiesel/diesel fuel blends. The addition of solketal and butyl diglycol to diesel/biodiesel blends yields positive results in terms of thermal efficiency. The highest thermal efficiency is 24.69% for D30B50S20 fuel at an engine torque of 11.1 Nm. The highest thermal losses occur in the D50B50 fuel mixture, which has the highest fuel energy among the fuels used in this study. Therefore, its thermal efficiency is low.

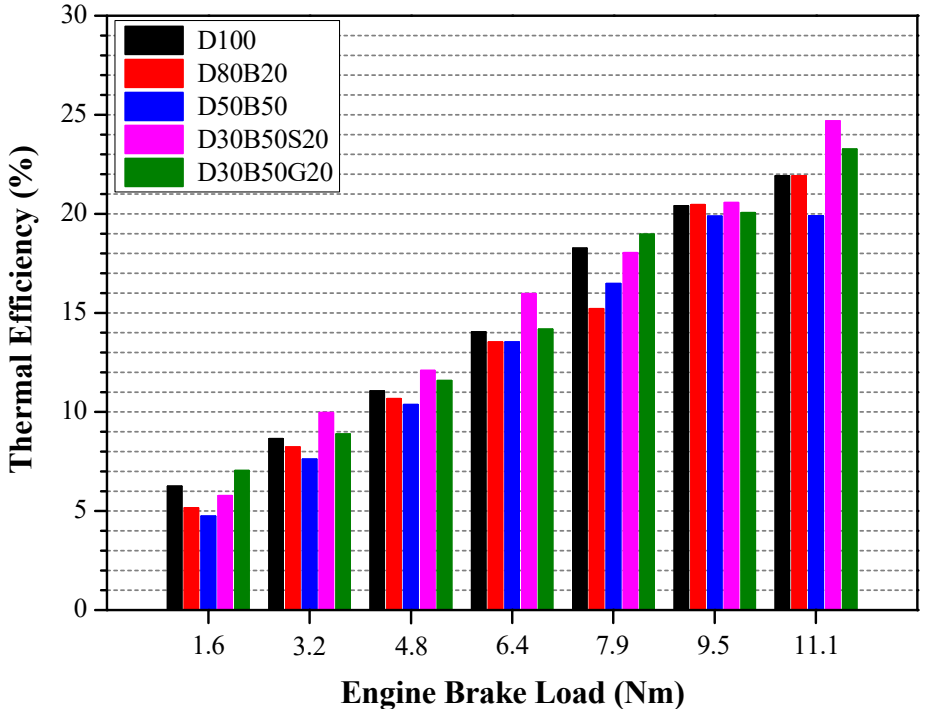

Figure 13. The variation in the thermal efficiency of fuel blends at different engine brake loads.

The chemical exergy of the fuel blends is given in Table 6. The highest exergy flow was calculated as 23.446 kW for the D50B50 fuel at an engine torque of 11.1 Nm. In D30B50G20 and D30B50S20 fuel blends formed by the addition of solketal and butyl diglycol to diesel/biodiesel fuel blends, a lower exergy flow was calculated compared to D100 fuel at all engine torques except 1.6 Nm and 7.9 Nm. D50B50 fuel showed an approximately 2–8% higher exergy flow than D80B20 fuel at all engine torque values except 6.4 Nm and 7.9 Nm. The highest exergy flow is 23.44 kW at an engine torque of 11.1 Nm for D50B50 fuel.

Table 6. The chemical exergy flows of fuel mixtures.

Engine Brake Load (Nm)	Exergy Flow (kW)				
	D100	D80B20	D50B50	D30B50S20	D30B50G20
1.6	10.803	12.964	14.090	11.583	9.263
3.2	15.600	16.236	17.492	13.437	14.675
4.8	18.287	18.791	19.295	16.625	16.858
6.4	19.228	19.759	19.693	16.780	18.370
7.9	18.461	21.964	20.216	18.571	17.163
9.5	19.831	19.591	20.115	19.537	19.464
11.1	21.544	21.338	23.446	18.983	19.583

In this study, the total exergy loss was calculated as the sum of the exhaust exergy of the fuel blends and the exergy losses due to heat transfer, and the values are given in Figure 14. D50B50 fuel showed the highest total exergy losses at all brake powers. D30B50S20 and D30B50G20 fuels have lower total exergy losses at all brake powers than other fuel blends. The lowest total exergy loss is 2.63 kW for D30B50G20 fuel at an engine torque of 1.6 Nm.

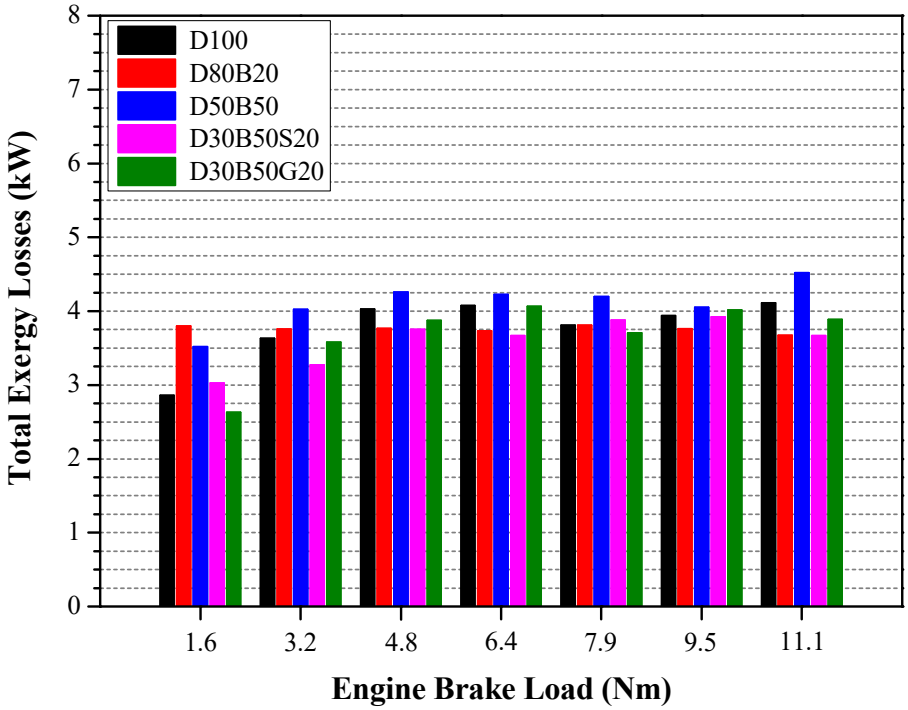

Figure 14. The variation in the total exergy losses of fuel blends at different engine brake loads.

The entropy production of fuel blends based on exergy destruction is calculated and given in Table 7. The highest entropy production was calculated as 0.052 kW/K for D50B50 fuel at an engine torque of 11.1 Nm. D30B50S20 and D30B50G20 fuels have the lowest values in entropy production at all engine brake powers. This indicates that the addition of solketal and butyl diglycol to fuel blends is exergetically favorable.

Table 7. Entropy generation.

Engine Brake Load (Nm)	Entropy Generation (kW/K)				
	D100	D80B20	D50B50	D30B50S20	D30B50G20
1.6	0.025	0.031	0.034	0.027	0.021
3.2	0.037	0.038	0.042	0.031	0.034
4.8	0.043	0.044	0.045	0.038	0.039
6.4	0.044	0.045	0.045	0.037	0.041
7.9	0.041	0.050	0.045	0.041	0.037
9.5	0.043	0.042	0.044	0.042	0.042
11.1	0.047	0.046	0.052	0.040	0.041

The most important output of exergy analysis is the exergy efficiency. The exergy efficiencies of the fuel mixtures used in this study are given in Figure 15. For all fuel blends, the exergy efficiency is lower than the thermal efficiency. This is because the exergy flow of fuels is higher than the energy flow. Among the fuel blends, the exergy efficiency of the fuels

with added solketal and butyl diglycol is higher than the other fuels. In diesel–biodiesel binary-fuel blends, exergy efficiency varies according to the D100 fuel. The highest exergy efficiency is 18.43% for D30B50S20 fuel at an engine torque of 11.1 Nm.

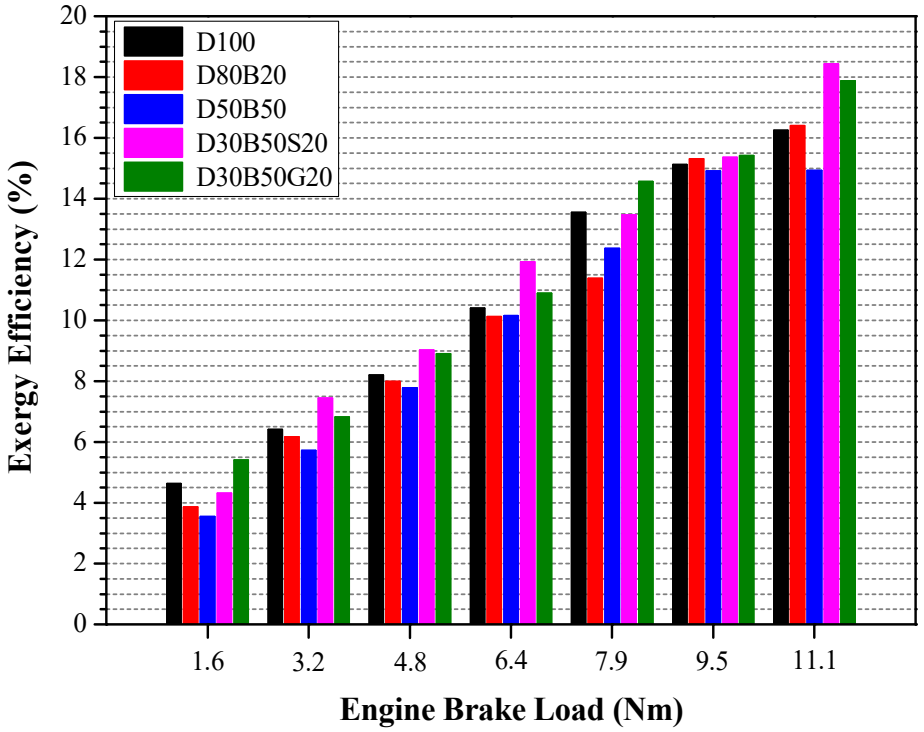

Figure 15. The variation in the exergy efficiency of fuel blends at different engine brake loads.

4. Conclusions

In this study, tests were carried out at seven different engine torques at a constant engine speed of 3000 rpm in a compression-ignition engine using five different fuel blends. Lower in-cylinder pressure values were obtained in the dual- and triple-fuel blends used in this study compared to D100 fuel. The lowest in-cylinder pressure values were observed in D50B50 fuel. The fuels obtained with the addition of solketal and butyl diglycol to the blends showed a decrease in in-cylinder pressure values compared to D100 fuel. After D100 fuel, the highest heat generation occurred in the oxygen-rich D30B50G20 fuel. Exhaust gas temperatures were found to increase with the addition of solketal and butyl diglycol to diesel-biodiesel blends. The highest exhaust gas temperature was 443 °C for D30B50G20 fuel.

The addition of solketal and butyl diglycol to fuel blends causes CO, HC, and smoke opacity emissions to decrease and CO_2 emissions to increase. In this study, the lowest CO emission was measured as 0.02% in D30B50G20 fuel at engine torques of 1.6 Nm and 11.1 Nm. At an engine torque of 11.1 Nm, HC emissions of 95 ppm and 19 ppm were measured for D100 and D30B50E20 fuels, respectively.

D30B50S20 and D30B50G20 fuel blends showed the best performance in thermal efficiency and exergy efficiency. At an engine torque of 11.1 Nm, the highest thermal and exergy efficiencies of D30B50S20 fuel were calculated as 24.69% and 18.44%, respectively.

As a result of engine performance and emission tests and thermodynamic analyses, it is evaluated that the addition of solketal and butyl diglycol to diesel/biodiesel fuel blends is appropriate. In future studies, it would be appropriate to carry out economic analyses of solketal and butyl diglycol and to give importance to studies to increase production capacity for fuel purposes.

Funding: The authors declare that no funds, grants, or other support were received during the preparation of this manuscript.

Institutional Review Board Statement: The authors confirm that they have complied with all ethical rules in all experimental studies.

Informed Consent Statement: Not applicable.

Data Availability Statement: The data of the study can be obtained upon special request.

Conflicts of Interest: The authors declare no conflict of interest.

Nomenclature

BSFC	Brake-specific fuel consumption (g/kWh)
BTE	brake thermal efficiency
$C_{15}H_{25}$	diesel
CA	crank angle
CD	combustion duration (°CA)
CHR	cumulative heat release (J)
CI	Compression ignition
CO	carbon monoxide
CO_2	carbon dioxide
Cp	in-cylinder pressure (bar)
DI	Direct injection
D100	100% diesel
D80B20	80% diesel and 20% biodiesel
D50B50	50% diesel and 50% biodiesel
D30B50S20	30% diesel, 50% biodiesel, and 20% solketal
D30B50G20	30% diesel, 50% biodiesel, and 20% butyl diglycol
EOC	end of combustion (°CA)
HC	hydrocarbon
HRR	heat release rate (J/°CA)
H_2O	water
ICE	internal combustion engine
ID	Ignition delay
NO_X	nitrogen oxide
O_2	oxygen
RoPR	rate of pressure rise (bar/°CA)
TDC	top dead center

References

1. Wang, J.; Azam, W. Natural resource scarcity, fossil fuel energy consumption, and total greenhouse gas emissions in top emitting countries. *Geosci. Front.* **2024**, *15*, 101757. [CrossRef]
2. Yi, S.; Abbasi, K.R.; Hussain, K.; Albaker, A.; Alvarado, R. Environmental concerns in the United States: Can renewable energy, fossil fuel energy, and natural resources depletion help? *Gondwana Res.* **2023**, *117*, 41–55. [CrossRef]
3. Abbasi, K.R.; Shahbaz, M.; Zhang, J.; Irfan, M.; Alvarado, R. Analyze the environmental sustainability factors of China: The role of fossil fuel energy and renewable energy. *Renew. Energy* **2022**, *187*, 390–402. [CrossRef]
4. Li, B.; Haneklaus, N. The role of renewable energy, fossil fuel consumption, urbanization and economic growth on CO_2 emissions in China. *Energy Rep.* **2021**, *7*, 1016–1024. [CrossRef]
5. Chen, X.H.; Tee, K.; Elnahass, M.; Ahmed, R. Assessing the environmental impacts of renewable energy sources: A case study on air pollution and carbon emissions in China. *J. Environ. Manag.* **2023**, *345*, 118525. [CrossRef]
6. Ma, Q.; Zhang, Q.; Liang, J.; Yang, C. The performance and emissions characteristics of diesel/biodiesel/alcohol blends in a diesel engine. *Energy Rep.* **2021**, *7*, 904–915. [CrossRef]
7. Karami, R.; Rasul, M.G.; Khan, M.M.K.; Salahi, M.M. Experimental and computational analysis of combustion characteristics of a diesel engine fueled with diesel-tomato seed oil biodiesel blends. *Fuel* **2021**, *285*, 119243. [CrossRef]

8. Öztürk, E.; Can, Ö.; Usta, N.; Yücesu, H.S. Effects of retarded fuel injection timing on combustion and emissions of a diesel engine fueled with canola biodiesel. *Eng. Sci. Technol. Int. J.* **2020**, *23*, 1466–1475. [CrossRef]
9. Sathyamurthy, R.; Balaji, D.; Gorjian, S.; Muthiya, S.J.; Bharathwaaj, R.; Vasanthaseelan, S.; Essa, F.A. Performance, combustion and emission characteristics of a DI-CI diesel engine fueled with corn oil methyl ester biodiesel blends. *Sustain. Energy Technol. Assess.* **2021**, *43*, 100981. [CrossRef]
10. Wang, Y.; Ou, S.; Liu, P.; Zhang, Z. Preparation of biodiesel from waste cooking oil via two-step catalyzed process. *Energy Convers. Manag.* **2007**, *48*, 184–188.
11. Geng, L.; Bi, L.; Li, Q.; Chen, H.; Xie, Y. Experimental study on spray characteristics, combustion stability, and emission performance of a CRDI diesel engine operated with biodiesel–ethanol blends. *Energy Rep.* **2021**, *7*, 904–915. [CrossRef]
12. Yeşilyurt, M.K.; Arslan, M. Analysis of the fuel injection pressure effects on energy and exergy efficiencies of a diesel engine operating with biodiesel. *Biofuels* **2019**, *10*, 643–655. [CrossRef]
13. Zheng, Z.; Li, C.; Liu, H.; Zhang, Y.; Zhong, X.; Yao, M. Experimental study on diesel conventional and low-temperature combustion by fueling four isomers of butanol. *Fuel* **2015**, *141*, 109–119. [CrossRef]
14. Kumar, S.; Dinesha, P.; Ajay, C.M.; Kabbur, P. Combined effect of oxygenated liquid and metal oxide nanoparticle fuel additives on the combustion characteristics of a biodiesel engine operated with higher blend percentages. *Energy* **2020**, *197*, 117194. [CrossRef]
15. Kumar, P.; Kumar, S.; Shah, S.; Kumar, S. Study of performance parameters and emissions of four-stroke CI engine using solketal-biodiesel blends. *SN Appl. Sci.* **2021**, *3*, 59. [CrossRef]
16. Chang, Y.C.; Lee, W.J.; Wu, T.S.; Wu, C.Y.; Chen, S.J. Use of water containing acetone–butanol–ethanol for NOx-PM (nitrogen oxide-particulate matter) trade-off in the diesel engine fueled with biodiesel. *Energy* **2014**, *64*, 678–687. [CrossRef]
17. Jamrozik, A.; Tutak, W.; Grab-Rogaliński, K. Effects of Propanol on the Performance and Emissions of a Dual-Fuel Industrial Diesel Engine. *Appl. Sci.* **2022**, *12*, 5674. [CrossRef]
18. Masera, K.; Hossain, A.K.; Davies, P.A.; Doudin, K. Investigation of 2-butoxyethanol as biodiesel additive on fuel property and combustion characteristics of two neat biodiesels. *Renew. Energy* **2021**, *164*, 285–297. [CrossRef]
19. Nabi, M.N.; Rasul, M.G. Influence of second-generation biodiesel on engine performance, emissions, energy and exergy parameters. *Energy Convers. Manag.* **2018**, *169*, 326–333. [CrossRef]
20. Zhu, M.; Cui, S.; Fang, J.; Zhong, Z.; Li, K.; Ai, X.; Wu, K.; Liang, B.; Wen, J. Exergy analysis-based operating parameter optimization for hydrogen energy hub. *Appl. Energy* **2025**, *38*, 5125491. [CrossRef]
21. Cai, X.; Guo, Z.; Wang, H.; Zhang, Y.; Ge, G.; Sun, X.; Sun, H.; Wang, H.; Li, R. A Thermodynamic Perspective on the Efficient Pressure Potential Energy Release in an Ice-Assisted Near-Isothermal Caes System. Available online: https://ssrn.com/abstract=5125925 (accessed on 20 January 2025).
22. Paul, A.; Panua, R.; Debroy, D. An experimental study of combustion, performance, exergy, and emission characteristics of a CI engine fueled by diesel-ethanol-biodiesel blends. *Energy* **2017**, *141*, 839–852. [CrossRef]
23. Madheshiya, A.K.; Vedrtnam, A. Energy-exergy analysis of biodiesel fuels produced from waste cooking oil and mustard oil. *Fuel* **2018**, *214*, 386–408. [CrossRef]
24. Kul, B.S.; Kahraman, A. Energy and exergy analyses of a diesel engine fueled with biodiesel-diesel blends containing 5% bioethanol. *Entropy* **2016**, *18*, 387. [CrossRef]
25. Hoseinpour, M.; Sadrnia, H.; Tabasizadeh, M.; Ghobadian, B. Energy and exergy analyses of a diesel engine fueled with diesel, biodiesel-diesel blend, and gasoline fumigation. *Energy* **2017**, *141*, 2408–2420. [CrossRef]
26. Şanli, B.G.; Uludamar, E. Energy and exergy analysis of a diesel engine fueled with diesel and biodiesel fuels at various engine speeds. *Energy Sources Part A Recovery Util. Environ. Eff.* **2020**, *42*, 1299–1313. [CrossRef]
27. Khoobbakht, G.; Akram, A.; Karimi, M.; Najafi, G. Exergy and energy analysis of combustion of blended levels of biodiesel, ethanol, and diesel fuel in a DI diesel engine. *Appl. Therm. Eng.* **2016**, *99*, 720–729. [CrossRef]
28. Mubarak, M.; Shaija, A.; Suchithra, T.V. Experimental evaluation of Salvinia molesta oil biodiesel/diesel blends fuel on combustion, performance, and emission analysis of diesel engine. *Fuel* **2021**, *287*, 119526. [CrossRef]
29. Gad, M.S.; Kamel, B.M.; Badruddin, I.A. Improving the diesel engine performance, emissions, and combustion characteristics using biodiesel with carbon nanomaterials. *Fuel* **2021**, *288*, 119665. [CrossRef]
30. Arias, S.; Molina, F.; Agudelo, J.R. Palm oil biodiesel: An assessment of PAH emissions, oxidative potential, and ecotoxicity of particulate matter. *J. Environ. Sci.* **2021**, *101*, 326–338. [CrossRef]
31. Alptekin, E. Emission, injection, and combustion characteristics of biodiesel and oxygenated fuel blends in a common rail diesel engine. *Energy* **2017**, *119*, 44–52. [CrossRef]
32. Özer, S. Effects of alternative fuel use in a vehicle with TSI (turbocharged direct-injection spark-ignition) engine technology. *Int. J. Green Energy* **2021**, *18*, 1309–1319. [CrossRef]
33. Doğan, B.; Özer, S.; Erol, D. Exergy, exergoeconomic, and exergoenviroeconomic evaluations of the use of diesel/fusel oil blends in compression ignition engines. *Sustain. Energy Technol. Assess.* **2022**, *53*, 102475. [CrossRef]

34. Taghavifar, H.; Nemati, A.; Walther, J.H. Combustion and exergy analysis of multi-component diesel-DME-methanol blends in HCCI engine. *Energy* **2019**, *187*, 115951. [CrossRef]
35. Özer, S.; Tunçer, E.; Demir, U.; Gülcan, H.E. Thermodynamic, thermoeconomic, and exergoeconomic analysis of a UAV two stroke engine fueled with gasoline-octanol and gasoline-hexanol blends. *Energy Convers. Manag.* **2025**, *327*, 119545. [CrossRef]
36. Dogan, B.; Erol, D.; Yaman, H.; Kodanli, E. The effect of ethanol-gasoline blends on performance and exhaust emissions of a spark ignition engine through exergy analysis. *Appl. Therm. Eng.* **2017**, *120*, 433–443. [CrossRef]
37. Ağbulut, Ü. Understanding the role of nanoparticle size on energy, exergy, thermoeconomic, exergoeconomic, and sustainability analyses of an IC engine: A thermodynamic approach. *Fuel Process. Technol.* **2022**, *225*, 107060. [CrossRef]
38. Doğan, B.; Erol, D. The investigation of energy and exergy analyses in compression ignition engines using diesel/biodiesel fuel blends-a review. *J. Therm. Anal. Calorim.* **2023**, *148*, 1765–1782. [CrossRef]
39. Rajpoot, A.S.; Chelladurai, H.; Choudhary, A.K.; Ambade, B.; Choudhary, T. Thermal and environmental assessment of Botryococcus braunii green biodiesel with nanoparticles using energy-exergy-emission-sustainability (3ES) analysis in a diesel engine. *Sustain. Energy Technol. Assess.* **2023**, *60*, 103473. [CrossRef]
40. Canakci, M.; Hosoz, M. Energy and exergy analyses of a diesel engine fuelled with various biodiesels. *Energy Sources Part B* **2006**, *1*, 379–394. [CrossRef]
41. Karami, S.; Gharehghani, A. Effect of nano-particles concentrations on the energy and exergy efficiency improvement of indirect-injection diesel engine. *Energy Rep.* **2021**, *7*, 3273–3285. [CrossRef]
42. Mishra, S.S.; Mohapatra, T. Energy-exergy-emission-economic performance and multi-response optimisation of a VCR CI engine using bio ethanol blended diesel fuel with Al_2O_3 nanoparticles. *Int. J. Exergy* **2023**, *41*, 74–90. [CrossRef]
43. Shadidi, B.; Alizade, H.H.A.; Najafi, G. Performance and exergy analysis of a diesel engine run on petrodiesel and biodiesel blends containing mixed CeO_2 and MoO_3 nanocatalyst. *Biofuels* **2022**, *13*, 1–7. [CrossRef]
44. Özcan, H. Energy and exergy analyses of Al_2O_3-diesel-biodiesel blends in a diesel engine. *Int. J. Exergy* **2019**, *28*, 29–45. [CrossRef]
45. Raja, S.; Natarajan, S.; Eshwar, D.; Alphin, M.S. Energy and exergy analysis and multi-objective optimization of a biodiesel fueled direct ignition engine. *Results Chem.* **2022**, *4*, 100284. [CrossRef]
46. Moran, M.J.; Shapiro, H.N.; Boettner, D.D.; Bailey, M.B. *Fundamentals of Engineering Thermodynamics*; John Wiley Sons: Hoboken, NJ, USA, 2010.
47. Channapattana, S.V.; Campli, S.; Madhusudhan, A.; Notla, S.; Arkerimath, R.; Tripathi, M.K. Energy analysis of DI-CI engine with nickel oxide nanoparticle added azadirachta indica biofuel at different static injection timing based on exergy. *Energy* **2023**, *267*, 126622. [CrossRef]
48. Jassim, E.I. Exergy analysis of petrol engine accommodated nanoparticle in the lubricant system. *Int. J. Exergy* **2021**, *35*, 406–420. [CrossRef]
49. Gad, M.S.; Aziz, M.M.A.; Kayed, H. Impact of different nano additives on performance, combustion, emissions and exergetic analysis of a diesel engine using waste cooking oil biodiesel. *Propuls. Power Res.* **2022**, *11*, 209–223. [CrossRef]
50. Gumus, M. A comprehensive experimental investigation of combustion and heat release characteristics of a biodiesel (hazelnut kernel oil methyl ester) fueled direct injection compression ignition engine. *Fuel* **2010**, *89*, 2802–2814. [CrossRef]
51. Akçay, M.; Yılmaz, İ.T.; Feyzioğlu, A. Effect of hydrogen addition on performance and emission characteristics of a common-rail CI engine fueled with diesel/waste cooking oil biodiesel blends. *Energy* **2020**, *212*, 118538. [CrossRef]
52. Raman, L.A.; Deepanraj, B.; Rajakumar, S.; Sivasubramanian, V. Experimental investigation on performance, combustion, and emission analysis of a direct injection diesel engine fuelled with rapeseed oil biodiesel. *Fuel* **2019**, *246*, 69–74. [CrossRef]
53. Bragadeshwaran, A.; Kasianantham, N.; Ballusamy, S.; Tarun, K.R.; Dharmaraj, A.P.; Kaisan, M.U. Experimental study of methyl tert-butyl ether as an oxygenated additive in diesel and *Calophyllum inophyllum* methyl ester blended fuel in CI engine. *Environ. Sci. Pollut. Res.* **2018**, *25*, 33573–33590. [CrossRef]
54. Kumar, C.; Rana, K.B.; Tripathi, B.; Nayyar, A. Properties and effects of organic additives on performance and emission characteristics of diesel engine: A comprehensive review. *Environ. Sci. Pollut. Res.* **2018**, *25*, 22475–22498. [CrossRef]
55. Killol, A.; Reddy, N.; Paruvada, S.; Murugan, S. Experimental studies of a diesel engine run on biodiesel n-butanol blends. *Renew. Energy* **2019**, *135*, 687–700. [CrossRef]
56. Tarabet, L.; Loubar, K.; Lounici, M.S.; Hanchi, S.; Tazerout, M. Eucalyptus biodiesel as an alternative to diesel fuel: Preparation and tests on DI diesel engine. *J. Biomed. Biotechnol.* **2012**, *2012*, 235485. [CrossRef]
57. El-Seey, A.I.; He, Z.; Hassan, H.; Balasubramanian, D. Improvement of combustion and emission characteristics of a diesel engine working with diesel/jojoba oil blends and butanol additive. *Fuel* **2020**, *279*, 118433. [CrossRef]
58. Yeşilyurt, M.K. A detailed investigation on the performance, combustion, and exhaust emission characteristics of a diesel engine running on the blend of diesel fuel, biodiesel, and 1-heptanol (C7 alcohol) as a next-generation higher alcohol. *Fuel* **2020**, *275*, 117893. [CrossRef]
59. Nour, M.; Attia, A.M.A.; Nada, S.A. Improvement of CI engine combustion and performance running on ternary blends of higher alcohol (Pentanol and Octanol)/hydrous ethanol/diesel. *Fuel* **2019**, *251*, 10–22. [CrossRef]

60. Papu, N.H.; Lingfa, P.; Dash, S.K. An experimental investigation on the combustion characteristics of a direct injection diesel engine fueled with an algal biodiesel. *Clean Technol. Environ. Policy* **2021**, *23*, 1769–1783. [CrossRef]
61. Geng, L.; Cheng, Y.; Chen, X.; Lee, C.F. Study on combustion characteristics and particulate emissions of a common-rail diesel engine fueled with n-butanol and waste cooking oil blends. *J. Energy Inst.* **2019**, *92*, 438–449. [CrossRef]
62. Ghadikolaei, M.A.; Wei, L.; Cheung, C.S.; Yung, K.F. Effects of engine load and biodiesel content on performance and regulated and unregulated emissions of a diesel engine using contour-plot map. *Sci. Total Environ.* **2019**, *658*, 1117–1130. [CrossRef]
63. Rajak, U.; Nashine, P.; Verma, T.N. Assessment of diesel engine performance using spirulina microalgae biodiesel. *Energy* **2019**, *166*, 1025–1036. [CrossRef]
64. Attia, A.M.A.; Kulchitskiy, A.R.; Nour, M.; El-Seesy, A.I.; Nada, S.A. The influence of castor biodiesel blending ratio on engine performance including the determined diesel particulate matters composition. *Energy* **2022**, *239*, 121951. [CrossRef]
65. Özer, S. The effect of adding toluene to increase the combustion efficiency of biodiesel. *Energy Sources Part A Recovery Util. Environ. Eff.* **2020**, *46*, 9325–9340. [CrossRef]
66. Karagöz, M.; Ağbulut, Ü.; Sarıdemir, S. Waste to energy: Production of waste tire pyrolysis oil and comprehensive analysis of its usability in diesel engines. *Fuel* **2020**, *275*, 117844. [CrossRef]
67. Verma, P.; Dwivedi, G.; Behura, A.K.; Patel, D.K.; Verma, T.N.; Pugazhendhi, A. Experimental investigation of diesel engine fueled with different alkyl esters of Karanja oil. *Fuel* **2020**, *275*, 117920. [CrossRef]
68. Behçet, R. Performance and emission study of waste anchovy fish biodiesel in a diesel engine. *Fuel Process. Technol.* **2011**, *92*, 1187–1194. [CrossRef]
69. Jaichandar, S.; Annamalai, K. Effects of open combustion chamber geometries on the performance of pongamia biodiesel in a DI diesel engine. *Fuel* **2012**, *98*, 272–279. [CrossRef]
70. Ramakrishnan, P.; Kasimani, R.; Peer, M.S.; Rajamohan, S. Assessment of n-pentanol/*Calophyllum inophyllum*/diesel blends on the performance, emission, and combustion characteristics of a constant-speed variable compression ratio direct injection diesel engine. *Environ. Sci. Pollut. Res.* **2018**, *25*, 13731–13744. [CrossRef]
71. Yilmaz, N.; Atmanli, A. Experimental assessment of a diesel engine fueled with diesel-biodiesel-1-pentanol blends. *Fuel* **2017**, *191*, 190–197. [CrossRef]
72. Babu, D.; Anand, R. Effect of biodiesel-diesel-n-pentanol and biodiesel-diesel-n-hexanol blends on diesel engine emission and combustion characteristics. *Energy* **2017**, *133*, 761–776. [CrossRef]
73. Hazrat, M.A.; Rasul, M.G.; Khan, M.M.K.; Ashwath, N.; Rufford, T.E. Emission characteristics of waste tallow and waste cooking oil-based ternary biodiesel fuels. *Energy Procedia* **2019**, *160*, 842–847. [CrossRef]
74. Amid, S.; Aghbashlo, M.; Tabatabaei, M.; Hajiahmad, A.; Najafi, B.; Ghaziaskar, H.S.; Rastegari, H.; Hosseinzadeh-Bandbafhaa, H.; Mohammadi, P. Effects of waste-derived ethylene glycol diacetate as a novel oxygenated additive on performance and emission characteristics of a diesel engine fueled with diesel/biodiesel blends. *Energy Convers. Manag.* **2020**, *203*, 112245. [CrossRef]
75. Gu, X.; Li, G.; Jiang, X.; Huang, Z.; Lee, C.F. Experimental study on the performance of and emissions from a low-speed light-duty diesel engine fueled with n-butanol-diesel and isobutanol–diesel blends. *Proc. Inst. Mech. Eng. Part D J. Automob. Eng.* **2013**, *227*, 261–271. [CrossRef]
76. Prabu, A.; Anand, R.B. Effects of oxygenate additive mixture on the performance and emission characteristics of a biodiesel-fueled compression ignition engine. *Aust. J. Mech. Eng.* **2019**, *17*, 8–13. [CrossRef]
77. Doğan, O. The influence of n-butanol/diesel fuel blends utilization on a small diesel engine performance and emissions. *Fuel* **2011**, *90*, 2467–2472. [CrossRef]
78. Baskar, P.; Senthilkumar, A. Effects of oxygen-enriched combustion on pollution and performance characteristics of a diesel engine. *Eng. Sci. Technol. Int. J.* **2016**, *19*, 438–443. [CrossRef]